



# Influence of Germination Time on the Morphological, Structural, Vibrational, Thermal and Pasting Properties of Potato Starch from *Solanum tuberosum* Phureja Group

Juan Carlos Lucas-Aguirre<sup>1</sup> · Víctor Dumar Quintero-Castaño<sup>1</sup> ·  
Johan Sebastián Henao-Ossa<sup>1</sup> · Oscar Yael Barrón-García<sup>2,3</sup> ·  
Mario Enrique Rodríguez-García<sup>2</sup>



Received: 6 February 2024 / Accepted: 2 August 2024  
© The Author(s) 2024

## Abstract

This work focuses on the study of the physicochemical changes that take place during a short germination period in flours and starches of the Creole potato tuber. To this end, the changes in the composition of flours and the structural, thermal, vibrational, functional and pasting changes of the isolated starches from germinated potatoes were evaluated during the 12-day germination period, measured every 4 days. The water absorption index (WAI) and the swelling powder showed no significant changes. Germination resulted in a decrease in fat and ash content, but an increase in protein and amylose content. Scanning electron microscopy (SEM) showed no changes in the morphology of the starch during germination. X-ray diffraction showed that isolated Creole potato starch contains nanocrystals with hexagonal crystal structure, which are not affected by germination. Differential scanning calorimetry (DSC) shows a shift of the gelatinization peak to the right, which could be attributed to the concentration effect. The pasting profiles of the isolated starches show no significant changes, indicating that the starch granules do not suffer any external damage due to the enzymatic process during germination and that the final viscosity behaves like a hydrogel.

**Keywords** Creole potato · Germination · Physicochemical properties · Starch · Structural analysis · Vibrational analysis

## Introduction

The potato, a staple food recognized by the Food and Agriculture Organization of the United Nations (FAO) as one of the “six healthy foods”, is grown in over 150 countries. While tetraploid potatoes are the most widespread worldwide, diploid genotypes such as the “Creole potato (*Solanum tuberosum*)” offer promising

---

Extended author information available on the last page of the article

potential. The Creole potato, which belongs to the *Solanum tuberosum* Phureja group, is characterized by its round tubers with yellow flesh and skin and originates from the southern Andean region of Colombia and northern Ecuador (Duarte-Delgado et al. 2021).

Potato tubers act as a sink organ that accumulates starch, reserve proteins and other metabolic products during formation. After formation, they enter a dormant phase in which germination is inhibited and which can last from days to months, depending on the variety and environmental conditions. Dormancy ends when the tubers transition from a sink to a source state, mobilizing reserves to support shoot growth. Prior to germination, the tubers are stored in a soilless environment at 10–15 °C and 80–85% relative humidity, initiating the first phase of plant development. During this period, metabolic dormancy is dissipating, and the processes that promote shoot development are intensified (Agrimonti et al. 2007; Grzesik et al. 2022).

Potatoes are primarily valued for their starch content but also provide high-quality proteins, dietary fibre, phenolic compounds, carotenoids and vitamin C. However, these contents strongly depend on the gene expressions and are highly dependent on the genotype and agroclimatic conditions (Thomas et al. 2021).

Sprouting tubers, grains and legumes enhances the activity of hydrolytic enzymes, which break down starch, fibre and proteins, improving digestibility and nutritional value. This process also increases the bioactivity of macronutrients, making sprouted grains valuable for functional foods. Studies have shown that sprouting alters physicochemical properties of starch, enhancing foaming capacity, reducing starch molecule size, improving bread quality and increasing the elongation of starch films for packaging (Li et al. 2017; Xu et al. 2019; Contreras-Jiménez et al. 2019; Xing et al. 2021; Rodríguez-García et al. 2021; Lucas-Aguirre et al. 2023; 2024).

Starch, the most common dietary carbohydrate, consists of linear and helical amylose and branched amylopectin, formed by the  $\alpha$ -condensation of D-glucose units, where the amylose-amylopectin ratio varies depending on the botanical source, which affects the physicochemical properties of starch (Li et al. 2017; Xu et al. 2019; Contreras-Jiménez et al. 2019; Xing et al. 2021; Rodríguez-García et al. 2021; Lucas-Aguirre et al. 2023; 2024). Esquivel-Fajardo et al. (2022) defined starch as micro- or submicron particles composed of different molecules, including two amylose and amylopectin molecules, fat, proteins, minerals, salts and others, but they included in this definition that starch is also composed of nanocrystals with two different crystal structures. They reported the presence of nanocrystals with orthorhombic crystal structure, which indicates that this starch can be called A-type. Starches, in which nanocrystals with hexagonal crystal structure are present, are referred to as B-type, and starches, in which nanocrystals with hexagonal and orthorhombic crystal structure are present, are referred to as C-type. However, A-type, B-type and C-type are not a polymorphism as described in several papers on starch. This new definition means that it is very important to define the effects of germination on these starch components as a function of germination time.

The presence of nanocrystals in different starches was demonstrated by Gong et al. (2016) using the acid isolation method and transmission electron microscopy (TEM). However, the identification of the crystalline phases was not reported.

Rodriguez-Garcia et al. (2021) proposed a powder diffraction file to identify both crystal structures. Concerning to the crystal identification of the X-ray patterns of potato, Velásquez-Herrera et al. (2017), Dündar et al. (2009) and Lee and Tae-Wha (2015) indicated that it has a B-type shape, which is the classification for starches containing nanocrystals with hexagonal crystal structure. Caceres et al. (2012) reported that the amylose content is generally below 20%. The results of thermal analysis show that the onset ( $T_o$ ) and peak ( $T_p$ ) temperatures were between 59.1–63.5 and 62.6–67.88 °C, respectively. The changes in gelatinization enthalpy were all around 21 J g<sup>-1</sup>.

The aim of this work was to evaluate the effect of germination on the proximate composition of flours and on the morphological, structural, vibrational, thermal and pasting properties of starches from the *Solanum tuberosum* Phureja group and to study the effects on their properties. The results of this study could suggest processing alternatives, especially in the development of fermented beverages.

## Materials and Methods

### Sample Obtention

The Creole potato variety Corpoica-Sol Andina was used in this study. First, a manual selection was carried out to exclude contamination and/or potatoes with phytosanitary problems. They were washed and disinfected for 5 min with a sodium hypochlorite solution at a concentration of 50 ppm to avoid problems with fungal infections during the germination process. The potatoes were then dried at 30 °C with forced hot air. For each day of the germination process analysis (0, 4, 8, 12 days), 250 g were weighed and stored in the dark at room temperature (20 °C) during the entire period to promote the germination process and observed as shown in Fig. 1. At the end of each germination timepoint, flour and starch were immediately extracted as described below.

To obtain flour from the sprouted tubers, the sprouted potatoes were sliced at the end of each germination timepoint (0, 4, 8 and 12 days of germination) and dried in a forced-air oven at 40 °C for 48 h. They were ground and the flours were sieved through a 100-mesh sieve and then packed in zip-lock bags under controlled conditions of temperature (20 °C) and relative humidity (70%) until remaining tests were carried out.

### Germination Rate

Sprouting of potatoes was defined as a bud  $\geq 2$  mm. The germination percentage was calculated according to Eq. 1.

$$\text{GR (\%)} = \frac{N_d}{N} \times 100\% \quad (1)$$

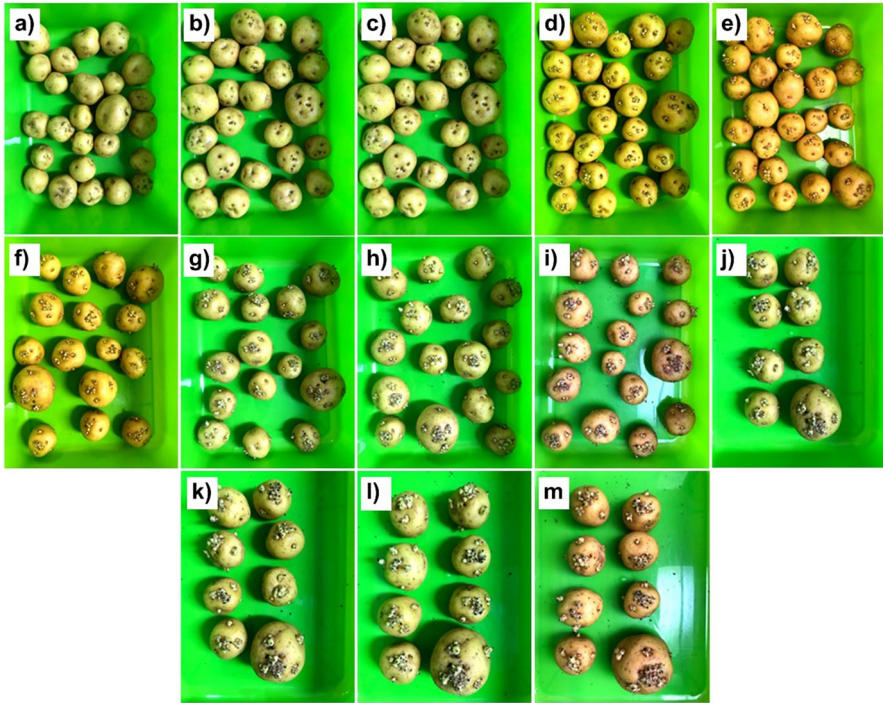


**Fig. 1** Images of Creole potato: **a** 0 days, **b** 1 day, **c** 2 days, **d** 3 days, **e** 4 days, **f** 5 days, **g** 6 days, **h** 7 days, **i** 8 days, **j** 9 days, **k** 10 days, **l** 11 days and **m** 12 days of germination

where  $N_d$  indicates the number of germinated eyes, and  $N$  is the total number of eyes that could germinate (Yang et al. 2023).

### Proximal Analysis of Flour from Fermented Tubers

For the proximate analysis of the Creole potato flours without germination (day 0) and with germination times of 4, 8 and 12 days, they were evaluated using the methods given by the AOAC International (2006), where the moisture content (method 925.10) was determined by the gravimetric method in an oven at 105 °C, until reaching constant weight; the fat (method 920.39) was determined by solid–liquid extraction (Soxhlet method); fibre (method 978.10) was determined by digestion with sulphuric acid and sodium hydroxide solutions and calcination of the residue; ash (method 942.05) was determined by calcination to constant weight, and protein (method 920.15) was determined by quantifying the total nitrogen content in the sample (Kjeldahl), with a factor of 6.25.

## Starch Isolation

Starch was isolated from potatoes at 0, 4, 8 and 12 days of germination using the method proposed by Gutiérrez-Cortez et al. (2021) and Rojas-Molina et al. (2024). In brief, 100 g of peeled potatoes were cut into cubes of 1 cm edge length and liquefied with 400 mL of distilled water for 3 min. To separate the starch, they were passed through a 100-mesh sieve, the starch was decanted at 4 °C for 12 h, the supernatant was removed, and to purify the starch, it was mixed with distilled water and then centrifuged at 2000 rpm to obtain isolated starch from each fraction. Subsequently, each fraction was dried in an oven at 40 °C for 48 h.

## Starch Content

The starch content of Creole potato flours at different germination times was quantified by the polarimetric method, following the methodology proposed by Gasiński and Kawa-Rygielska (2022).

## Amylose Content

The amylose content in ungerminated (0 days) and germinated (4, 8 and 12 days) isolated potato starch was determined using the spectrophotometric method (620 nm) based on the formation of the iodine-amylose complex formed by reacting dispersed and gelatinized starch granules quantified against a solution of known amylose concentration, after adjustment of a standard curve (Juliano et al. 1981).

## Scanning Electron Microscopy (SEM) of Potato Starch during Germination

SEM images of isolated Creole potato starch from ungerminated (0 days) and for each day of germination (4, 8 and 12 days) were studied in a scanning electron microscope (JEOL, JSM-6060LV-Japan) with HV mode resolution. The samples were coated with gold and fixed in a sample holder with carbon tape. The electron accelerating voltage was 20 kV at a pressure of 12–20 Pa (Quintero-Castaño et al. 2020).

## Particle Size Distribution

The mean particle size distribution of starch particles from ungerminated (0 days) and germinated (4, 8 and 12 days) Creole potato tubers was determined according to Mie's theory, using a refractive index of 1.52; the equipment used was a Mastersizer 3000 (Malvern Instrument Ltd., Worcestershire, UK), dispersing the

starch particles in 0.5 L of water, up to a darkening level of  $10 \pm 1\%$ , quantifying the D10, D50 and D90 percentiles (Lucas-Aguirre et al. 2018; 2019).

### **X-ray Diffraction Analysis**

To obtain the X-ray diffraction patterns, powder samples from ungerminated (0 days) and germinated (4, 8 and 12 days) Creole potato starches were taken and packed in an aluminium pan. A high-resolution diffractometer (Rigaku-Ultima 4, USA) was used to obtain the X-ray diffraction patterns. The measurements were taken at an angle of 5 to 35° on a scale of  $2\theta$ , with a  $\text{CuK}\alpha$  radiation wavelength of  $\lambda = 0.1540$  nm, at 35 kV and 15 mA (Quintero-Castaño et al. 2020).

### **Thermal Properties of Starch**

To measure the temperatures  $T_0$ ,  $T_p$ ,  $T_e$  and enthalpy of gelatinization of isolated starch from ungerminated (0 days) and germinated (4, 8 and 12 days) Creole potato tubers, samples ( $2.0 \pm 0.1$  mg) were hydrated with deionized water to 85% moisture (w/w); the heating profile was carried out from 30 to 120 °C, at a heating rate of 5.0 °C/min, using a previously calibrated DSC (Mettler Toledo, Greifensee, Switzerland) (Contreras-Jiménez et al. 2019).

### **Vibrational Analysis**

The vibrational analysis of isolated starches from ungerminated (0 days) and germinated (4, 8 and 12 days) Creole potatoes was characterized using an FTIR spectrophotometer (Perkin Elmer, Spectrum Two, USA) using attenuated total reflectance, recording the transmittance between 600 and 4000  $\text{cm}^{-1}$  (Contreras-Jiménez et al. 2019).

### **Pasting Properties**

The apparent viscosity profiles of isolated starches from ungerminated (0 days) and germinated (4, 8 and 12 days) Creole potatoes were determined using a modular compact rheometer (Anton Paar MCR 102, UK). A constant frequency of 193 rpm was used. The samples were heated for 5.3 min, from 50 to 92 °C, then held for 1 min and then cooled at the same rate to the initial temperature and held for 1 min (Rincón-Londoño et al. 2016).

### **Functional Properties of Starches**

A 2% (w/v) starch suspension was prepared, stirred and placed in a water bath at 90 °C for 30 min, then cooled and centrifuged at 2000 rpm for 20 min. The supernatant was removed and placed in an oven at 105 °C until constant weight was obtained. The respective weights were taken including the weight of the sediment,

and calculations were performed, determining the swelling power (SP), water solubility index (WSI) and water absorption index (WAI) (Contreras-Jiménez et al. 2019).

## Statistical Analysis

The tests were performed in triplicate, applying an analysis of variance with a significance level of 5% and Tukey's test, for the comparison of means using Statgraphics Centurion XVIII software.

## Results and Discussion

### Germination Rate

When dormancy is broken, germination begins. Figure 1 shows the images of Creole potatoes at different germination times and the rather irregular shape and size of harvested tubers. Germination is the most important visible milestone for determining the physiological age of the tuber. The first observable stage of germination is characterized by the appearance of small white buds, often referred to as “pipping” or “peeping” (Mani et al. 2014). As shown in Fig. 1e, which corresponds to day 4 of the germination process,  $37.8 \pm 2.45\%$  of the eyes have germinated, increasing to  $72.64 \pm 4.38\%$  on day 6 (Fig. 1i) and  $98.62 \pm 2.28\%$  (Fig. 1m) on day 12 of the germination process. These results agree with those of Yang et al. (2023), who worked with the potato variety *Solanum tuberosum* “Xisen no. 6” (Shepody  $\times$  XS9304). Finally, as apical dominance decreases, multiple sprouting gradually develops, characterized by the appearance of multiple buds sprouting along the tuber, with both the duration of apical dominance and the number of sprouts per tuber being a varietal trait (Mani et al. 2014).

### Proximate Analysis of Flours

Potato sprouting is a complex process involving several metabolic pathways as well as physiological and biochemical changes. Enzymatic reactions, carbohydrate metabolism and hormonal regulation are linked to the sprouting of potato tubers. Among the most important changes, the activity of enzymes related to sprouting gradually increases before sprouting, especially amylase activity, which rapidly increases during bud growth, and hydrolyzes starch to produce a large amount of sugar and energy for bud growth (Neupane et al. 2022; Yang et al. 2023). At the same time, some changes occur, such as the loss of weight, texture, nutritional value, softening, shrinkage and the formation of toxic alkaloids. Thus, in general, an average weight loss of  $3.16 \pm 1.00\%$  was observed in each of the studied potatoes during the 12 days of germination, as well as softening, shrinkage and wilting. Tuber weight loss during germination occurs through the periderm, and to a lesser extent through the lenticels (Mani et al. 2014).

**Table 1** Proximate composition of Creole potato flours as a function of the germination time

Time (days)	Fat (%)	Fibre (%)	Ash (%)	Protein (%)	Starch (%)	Moisture (%)	Amylose (%)
0	1.80 ± 0.11 <sup>c</sup>	3.79 ± 0.14 <sup>b</sup>	1.94 ± 0.11 <sup>b</sup>	3.67 ± 0.09 <sup>ab</sup>	77.32 ± 1.34 <sup>a</sup>	8.48 ± 0.17 <sup>c</sup>	22.96 ± 0.74 <sup>a</sup>
4	0.72 ± 0.04 <sup>b</sup>	3.11 ± 0.15 <sup>a</sup>	1.80 ± 0.14 <sup>b</sup>	3.57 ± 0.08 <sup>a</sup>	79.63 ± 2.03 <sup>b</sup>	7.97 ± 0.05 <sup>b</sup>	24.76 ± 1.2 <sup>ab</sup>
8	0.69 ± 0.02 <sup>b</sup>	3.20 ± 0.20 <sup>a</sup>	0.96 ± 0.06 <sup>a</sup>	4.37 ± 0.33 <sup>ab</sup>	80.97 ± 1.84 <sup>b</sup>	6.81 ± 0.09 <sup>a</sup>	27.56 ± 1.08 <sup>c</sup>
12	0.53 ± 0.01 <sup>a</sup>	3.06 ± 0.20 <sup>a</sup>	0.98 ± 0.02 <sup>a</sup>	4.47 ± 0.88 <sup>b</sup>	79.15 ± 0.95 <sup>b</sup>	8.81 ± 0.22 <sup>d</sup>	31.43 ± 0.94 <sup>d</sup>

Data are expressed as mean ± standard deviation (SD) from three replicates. Different letters in columns indicate significant differences ( $p < 0.05$ ) by Tukey's test

Table 1 shows the changes in the composition of Creole potato flour during germination process and shows statistically significant differences in the individual components as germination progresses ( $p < 0.05$ ). The most important changes include the decrease in fat (−70.56%), fibre (−19.26%) and ash (−49.48%) and the increase in protein (+21.8%) when comparing the values on day 0 with those on day 12 of germination.

During germination, the sprouts begin to grow after dormancy-break and form roots at their base. At this point, the tubers change from a storage organ to a source of nutrients and energy for the developing sprouts. The fat content decreases, which could be due to the fact that it is used as an energy source during the respiration process (Table 1), which is triggered by the tuber breaking its dormancy phase during post-harvest storage (Neupane et al. 2022). The same behaviour has also been observed in the germination of legumes such as lentils and peas (Lucas-Aguirre et al. 2023; 2024).

Tuber dormancy is controlled by phytohormones, which play an important role in triggering or inhibiting tuber dormancy in potatoes. All five major plant hormones are involved in this process: Abscisic acid and ethylene are involved in triggering dormancy; cytokinins are involved in breaking dormancy, and gibberellins and auxins are involved in sprout development. When potato dormancy is broken, the cellular balance is disturbed and a cascade of biochemical reactions is triggered, which include the migration of calcium ions into the meristems, increased cellular respiration and increased production of adenosine triphosphate (ATP), which could explain the decrease in minerals during the germination process (Table 1) (Mani et al. 2014). These responses could explain the appearance of apical and proximal buds and the decrease in membrane integrity in the tuber during germination.

According to the literature, the reactive oxygen species (superoxide anion, hydrogen peroxide and hydroxyl radicals) are also involved in the regulation of potato dormancy. The metabolism of hydrogen peroxide occurs in the mitochondria, in cortical tuber tissue since superoxide dismutase is activated (Mani et al. 2014). The moderate oxygenation of cells by hydrogen peroxide leads to an increase in intracellular  $\text{Ca}^{2+}$ , iron concentration and active entry into mitosis, triggering germination, while at the same time, the presence of hydrogen peroxide during germination acts on tuber protein metabolism. Indeed, germination is accompanied by protein carbonylation of the reserves, which makes them more sensitive to proteases and



proteolysis, as well as a decrease in the activity of the pentose phosphate pathway. This explains the depolymerization of starch to reducing sugars (glucose and fructose) in the potato tuber at the end of dormancy (Zabrouskov et al. 2002; Delaplace et al. 2008; Mani et al. 2014).

The starch content found in the flours of the Creole potato variety Corpoica-Sol Andina varied between 77.32 and 80.97% (Table 1). The results were higher than those obtained by Zarate-Polanco (2014), who worked with 17 promising clones, whose results varied between 45.23 and 72.98%. The proximate composition of the flours may depend on the type of tuber, cultivation practises, climate, soil type and the presence of pests and diseases, among other factors.

The results for percentage amylose content (Table 1) generally showed a similar behaviour to those reported by Cáceres et al. (2012), with starches from 24 diploid potato accessions of the Phureja group (19.7–25.8%) and of 2 commercial tetraploid potato cultivars of the *Solanum tuberosum* group (24–24.8%). Pineda-Gomez et al. (2021) reported amylose content between 29 and 40% for starch from six potato varieties (*Solanum tuberosum*) grown in the Andean region of southern Colombia, and Mueez-Ali et al. (2023) found amylose contents of native potato starches in the range 25.71–26.60%. It could be hypothesized that the Phureja starch has a lower ratio between short/long chains than the *S. tuberosum* starch, i.e. a higher proportion of long chains characteristic of amylopectin, which may have a major impact on the functional properties of the starch. At the same time, it is observed that the amylose content increases with increasing germination time, which is partly due to the conversion of amylopectin chains into amylose (Mueez-Ali et al. 2023).

### Morphological Changes in Isolated Potato Starch during the Germination Process

Figure 2a and b shows the morphological differences that occur in the starch grains of Creole potatoes. The small grains have a round shape and are on average  $181.88 \pm 28.13 \mu\text{m}$  long at their longest point, while the larger ones have an ovoid and/or elliptical shape and are on average  $375.08 \pm 87.45 \mu\text{m}$  long at their longest point. In general, the starch granules have a smooth, homogeneous and slightly uneven surface. At the same time, smaller circular round particles corresponding to protein molecules with an average diameter of  $38.69 \pm 11.11 \mu\text{m}$  can be seen on the SEM images (enclosed in yellow circles) (Fig. 2a–h).

The same attributes were reported by Choi et al. (2020) in potato starch (*Solanum tuberosum* L.), in which all samples showed a similar morphology, round, oval or elliptical, with a mixture of large, medium and small starch granule, and a shiny surface with a regular pattern. Small granules were mostly spherical, while large granules have an ellipsoidal shape (Cáceres et al. 2012).

When analyzing the possible effects of the germination process through the enzymatic activity on the integrity of the Creole potato starch granules (Fig. 2c–h), their surface does not change throughout the process. This fact indicates that the starch grains are not altered during the germination process, which leads to the development of fat, protein, stems and roots.

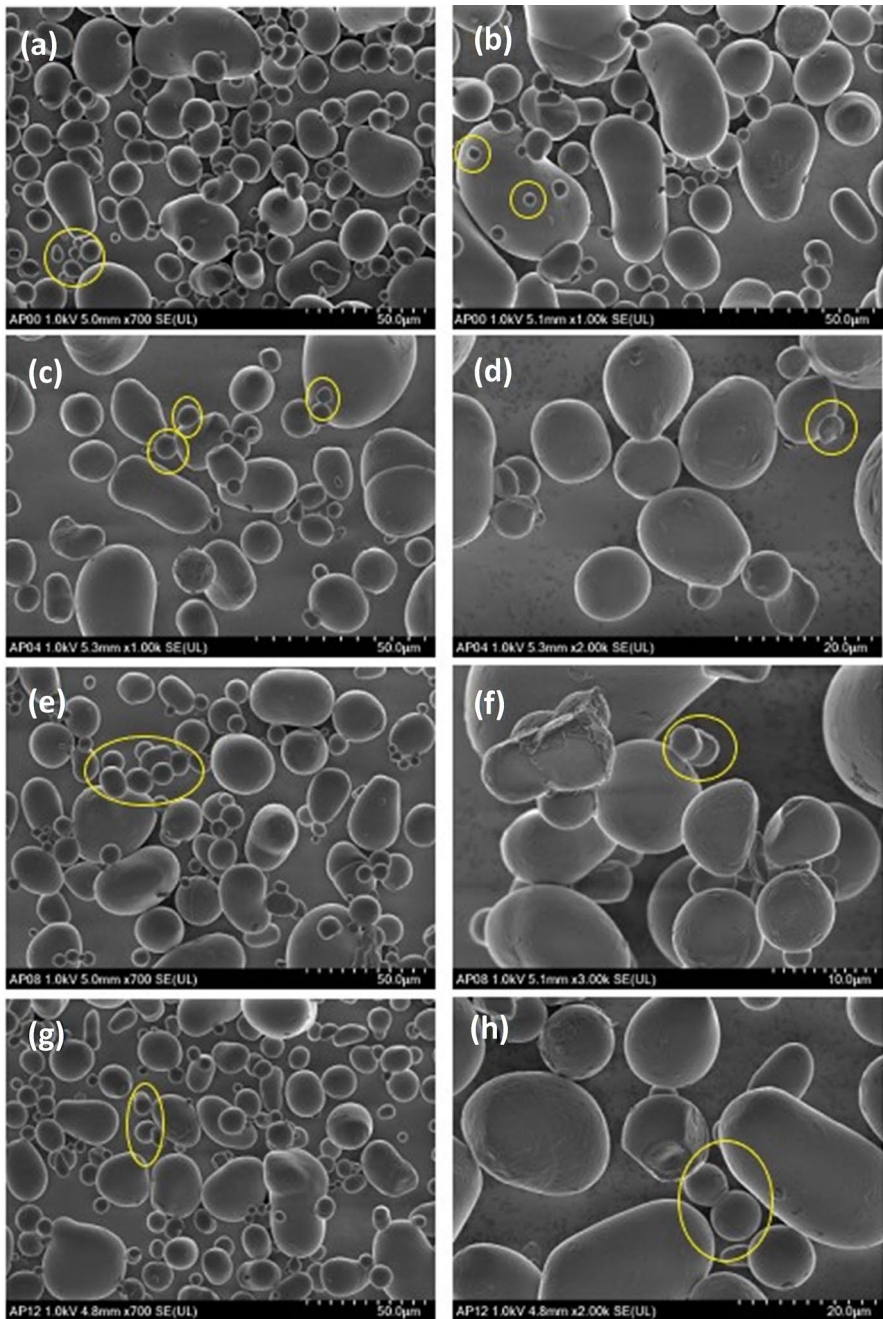


**Fig. 2** Microstructural changes of isolated Creole potato starch at different germination times. Day 0 (**a**, **b**), 4 days (**c**, **d**), 8 days (**e**, **f**) and 12 days (**g**, **h**) of germination (the structures enclosed in yellow circles correspond to protein molecules)

The most representative change in the starch granules during the germination process initially was the increase in the average diameter of the starch granules of Creole potato in the D90 percentile, manifesting as superficial and spongy erosion of the granules and formation of superficial pores in them; these changes could be associated to the enzymatic hydrolysis that penetrates the interior of the granules from the heliolic region towards the exterior, while in the D10 and D50 percentiles, the average diameter of the granules decreased (Lucas-Aguirre et al. 2024).

### Functional Properties of Isolated Potato Starch during Germination

In general, the germinated starch of Creole potato was found to have high WAI (g gel/g sample) ( $11.86 \pm 0.52$ – $10.43 \pm 0.11$ ) and SP (%) ( $12.07 \pm 0.55$ – $10.61 \pm 0.10$ ) and low values for WSI (%) ( $2.58 \pm 0.21$ – $1.79 \pm 0.15$ ) (Table 2), indicating that it is a good quality starch. The WAI decreased by 12.06% as the germination time progressed, while the SP decreased by 12.1%, which is consistent with the results of the rapid visco analyzer (RVA) tests (Fig. 5), where the peak viscosity decreases with increasing germination time. This could be due to the hydroxylation of amylose and amylopectin, which leads to a decrease in peak and final viscosity and causes the paste to behave like a hydrogel.

It is known that starch can reversibly absorb water before heating, but when the temperature rises close to the gelatinization temperature, water absorption is irreversible. This property indicates the ability of the granules to swell and quickly reach the viscosity peak, while the WAI measures the swelling capacity which depends on the availability of hydrophilic groups and the ability of the macromolecule to form a gel. On the other hand, the WSI is related to the number of soluble solids, and the WAI is mainly related to the damage of the starch and the presence of compounds other than starch, e.g. minerals (Pineda-Gómez et al. 2021).

Pineda-Gómez et al. (2021) reported very low WAI and WSI values in six potato starches of the genus *Solanum tuberosum*, where WAI values ranged from 1.95 to 2.39 g/g, while WSI ranged from 0.31 to 1.28%, relatively low values compared to the starches of the Phureja group, where they found that the apparent swelling of starch granules is a property mainly attributed to amylopectin. However, the mineral content in the starch may contribute to the water absorption capacity and therefore affect other physical properties such as viscosity development. The low solubility

**Table 2** Functional properties and particle size distribution of germinated Creole potato starch at different days of germination

Time (days)	WAI g (g gel/g sample)	WSI (%)	SP (%)	D10 (μm)	D50 (μm)	D90 (μm)
0	$11.86 \pm 0.52^b$	$2.46 \pm 0.11^{bc}$	$12.07 \pm 0.55^b$	$22.47 \pm 2.68^b$	$25.68 \pm 8.18^a$	$45.71 \pm 5.99^a$
4	$10.83 \pm 0.17^a$	$2.29 \pm 0.11^b$	$11.00 \pm 0.17^a$	$22.57 \pm 2.78^b$	$35.67 \pm 3.35^b$	$59.33 \pm 5.31^b$
8	$11.07 \pm 0.94^{ab}$	$1.79 \pm 0.15^a$	$11.21 \pm 0.96^{ab}$	$20.67 \pm 0.75^{ab}$	$38.33 \pm 9.85^b$	$69.00 \pm 4.38^c$
12	$10.43 \pm 0.11^a$	$2.58 \pm 0.21^c$	$10.61 \pm 0.10^a$	$18.12 \pm 0.33^a$	$40.33 \pm 9.21^{bc}$	$70.22 \pm 7.34^c$

Data are expressed as mean  $\pm$  standard deviation (SD) from three replicates. Different letters in columns indicate significant differences ( $p < 0.05$ ) by Tukey's test

at low temperatures could be attributed to the crystalline structure of starch and the presence of hydrogen bonds between -OH groups within the starch molecules. In addition, the solubility index tends to increase when the gelatinization temperature of the starch is exceeded.

### Structural Characterization

Figure 3 shows the X-ray diffraction patterns of isolated starch from Creole potato during the germination period. Rodríguez-García et al. (2021) have indexed the patterns for nanocrystals with hexagonal crystal structure. The dashed line in these patterns corresponds to the identification of this structure.

Therefore, the isolated starch from Creole potato can be classified as B-type (hexagonal crystal structure) and is consistent with the report by Velásquez-Herrera et al. (2017) for native potato starch. As can be observed, germination does not cause any significant change in the crystalline structure of these starch grains, which means that the enzymatic process does not affect the nanocrystals with hexagonal crystal structure. It is possible that during germination, the potato uses only the hydrolyzed amylose and amylopectin or part of the fat and proteins as the main energy source

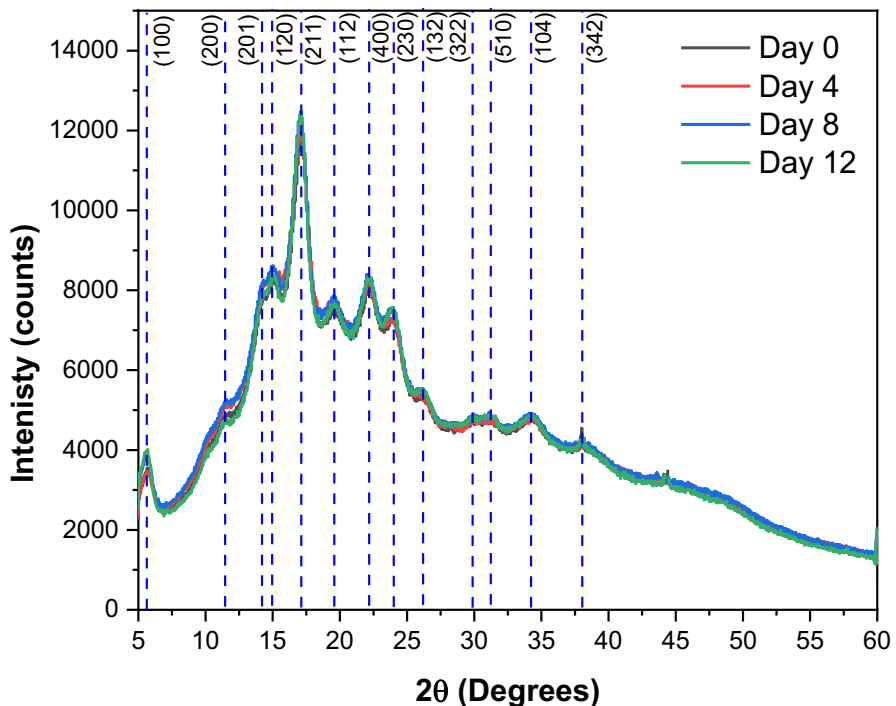


**Fig. 3** X-ray diffraction patterns of isolated Creole potato starch at different times of germination (0, 4, 8 and 12 days)

and that under the conditions of germination, the plant does not need the energy reservoir in the hexagonal crystals.

On the other hand, it is important to note that these X-ray patterns show broad peaks related to the presence of nanocrystals that generate elastic and inelastic scattering simultaneously (Londoño-Restrepo et al. 2018). The behavior of the nanocrystals along the germination time is still an open problem because in this case, the potato was germinated in dark conditions, a similar situation when the creole potato is planted a few centimeters deep. The use of all energy sources contained in the starch is limited by the beginning of the photosynthetic process in the leaves, which produce starch in the plant and prevent the use of the reserves (nanocrystals) contained in the mother seeds.

Table 3 shows the Miller indices, Bragg angles and interplanar spacing for the hexagonal crystal structure of Creole potato starch. Miller indices are a notation system in crystallography for planes in crystal (lattice) structures. These indices are used to describe the orientation of atomic planes in a crystal lattice. Bragg angles, also known as Bragg diffraction angles, are the specific angles at which X-rays are diffracted by the atomic planes in a crystal. These angles are determined by Bragg's law, which relates the wavelength of the incident wave, the spacing between the crystal planes and the angle of incidence at which constructive interference occurs. Using Table 3, and with the help of the reports of Rodríguez-García et al. (2021), it is possible to identify each of the diffraction peaks allowed for hexagonal crystal structure.

### Vibrational Analysis

Figure 4 shows the IR spectra obtained from the isolated starches during the germination process. The main components of the starch do not change and the

**Table 3** Miller indices ( $hkl$ ), Bragg angles ( $2\theta$ ) and interplanar spacing ( $d(\text{Å})$ ) for the hexagonal crystal structure in Creole potato starch

$hkl$	This work ( $2\theta$ )	Reported* Hexagonal ( $2\theta$ )	Reported* $d(\text{Å})$
(100)	5.6270	5.5056	16.0388
(200)	11.4581	11.0240	8.0194
(201)	14.2043	13.8500	6.3888
(120)	14.9567	14.6003	6.0621
(211)	17.1261	16.8462	5.2586
(112)	19.5839	19.3220	4.5900
(400)	22.1797	22.1516	4.0097
(230)	24.0105	24.1679	3.6796
(132)	26.1924	26.1631	3.4033
(322)	29.8792	29.5572	3.0198
(510)	31.2335	31.0195	2.8807
(104)	34.2305	34.3669	2.6074
(342)	38.0426	38.1101	2.3594

\*Rodríguez-García et al. (2021)

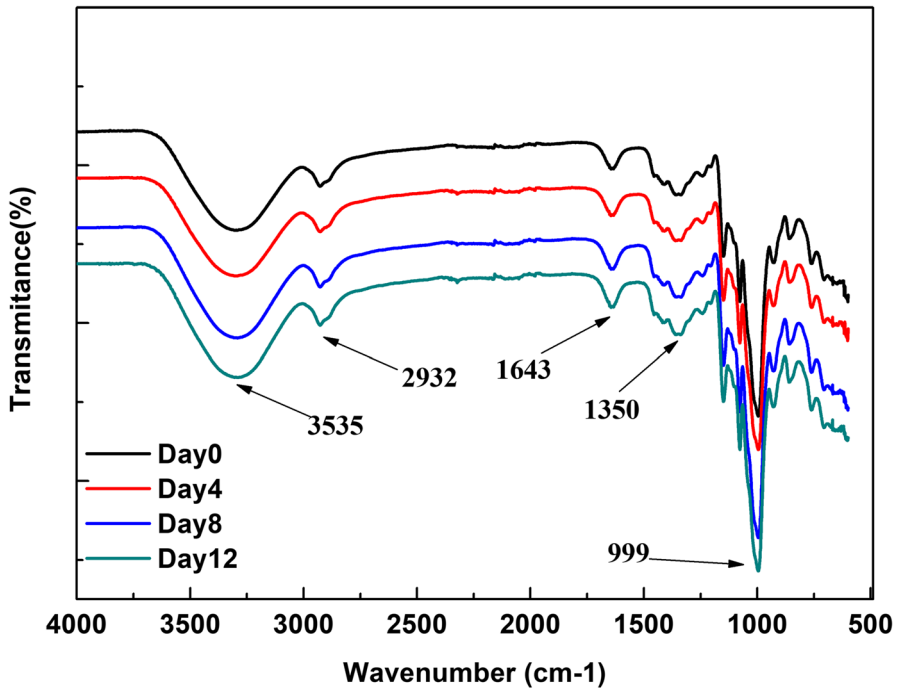


Fig. 4 FTIR spectra of the isolated Creole potato starch on different days of germination

formation of new compounds because of the starch germination process is not observed, which could be related to the lack of proteins and fats in the starch.

In general, the absorption band in the region around  $3350\text{ cm}^{-1}$  in starches corresponds to the symmetric and asymmetric stretching of intra- and intermolecular hydroxyl groups. The band observed around  $2900\text{ cm}^{-1}$  is related to the stretching of C-H bonds. During germination, changes occur in the starch granules, which are triggered by the enzymatic process. This creates sugar chains that are used by the grain as a source of carbon and energy for growth (Contreras-Jiménez et al. 2019). Figure 4 shows changes in the vibrational spectrum of starch between  $1700$  and  $1200\text{ cm}^{-1}$ , with the  $1643\text{ cm}^{-1}$  band corresponding to the carbonyl groups (Mueez-Ali et al. 2023). In the range between  $1350$  and  $1275\text{ cm}^{-1}$ , weakening is observed in the bands corresponding to the carbonyl group, possibly due to changes in the  $\alpha(1-4)$  and  $\alpha(1-6)$  glycosidic linkage. Similar results were reported by Daneri et al. (2016) and Contreras et al. (2019) in malted barley, showing that significant changes occur in the starch granules during malting. The main changes in these starches during germination are in the bands between  $3280-3350\text{ cm}^{-1}$  and between  $980-1040\text{ cm}^{-1}$  corresponding to the O-H bonds and the anhydrous glucose ring, respectively, increasing the intensity of the peaks (Fig. 4).

## Thermal Analysis

Gelatinization is perhaps the most important property to consider when processing starch. It is a transition from order to disorder in the internal structure of the grains and is very sensitive to the presence of plasticizers such as water. Esquivel-Fajardo et al. (2022) indicate that this transition can be in part caused by the solvation of the nanocrystals with hexagonal or orthorhombic crystal structures. The transition temperatures and enthalpy change due to the changes in these nanocrystals. The peak temperature ( $T_p$ ) in some cases be regarded as the point at which gelatinization is complete. The energy required for gelatinization can be measured by enthalpy ( $\Delta H$ ) and is indicated by the area under the curve in the DSC thermogram and is also an indicator of the molecular changes within the granules that occur during gelatinization (Pineda-Gómez et al. 2021).

Figure 5 shows the DSC results of the germinated starch of the Creole potato, where a slight increase in peak temperature ( $T_p$ ) can be observed with increasing germination time. The  $T_p$  values are between 62.2 and 62.6 °C from 0 to 4 days after germination. However, after 8 and 12 days of germination, the  $T_p$  value increases to 63.2 °C and 63.8 °C, respectively. These results could be due to the accumulation of sugars during germination. This discrepancy in gelatinization temperature after germination could be due to differences in germination conditions and plant sources (Wu et al. 2013), while enthalpy showed the same behaviour: it increased with increasing starch germination time but required less energy to achieve gelatinization

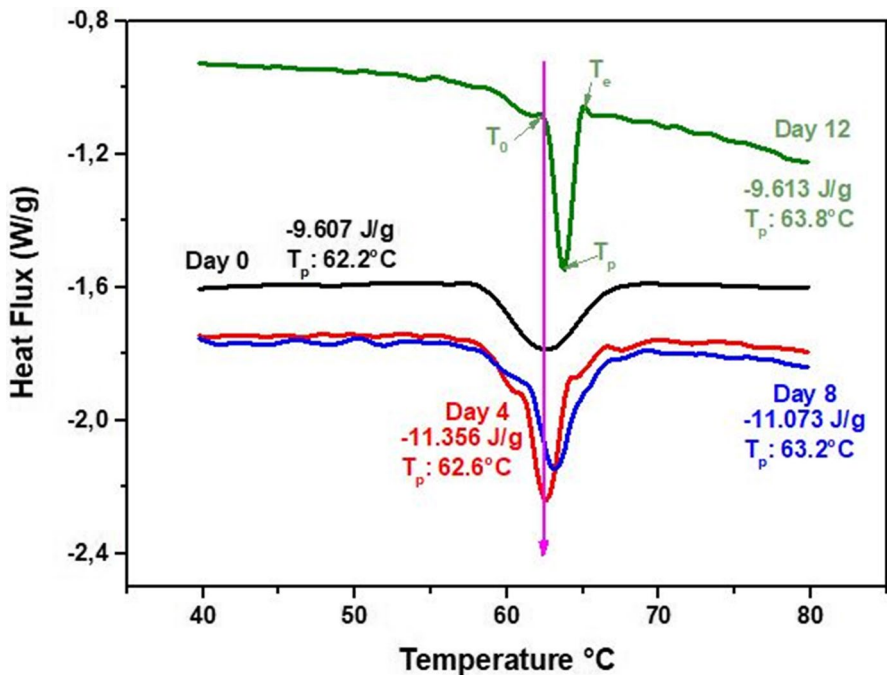


Fig. 5 DSC for isolated starches during germination time

of starch granules at day 12 (Fig. 5). This behaviour could be due to weakly associated double helices in non-crystalline regions, while the decrease in gelatinization enthalpy could be due to the lower proportion of longer branched chains that could form a shorter double helix order, leading to a decrease in gelatinization enthalpy (Wu et al. 2013).

These values determined for  $T_p$  were comparable with those of other studies, while the gelatinization enthalpies differed significantly. In Cáceres et al. (2012), working with 24 diploid accessions of the Phureja group, the  $T_p$  values ranged between 62.6 and 67.88 °C and the changes in gelatinization enthalpy varied very little in a range between 19.4 and 22.0 J g<sup>-1</sup>. At the same time, they report that they found no significant differences between the thermal properties of Phureja and *S. tuberosum* starches. Granule crystallinity increases with amylopectin, and the enthalpy of gelatinization ( $\Delta H$ ) from DSC analysis gives a general quantitative and qualitative measure of crystallinity, which is an indicator of the loss of molecular order within the grains.

Choi et al. (2020) and Pineda-Gómez et al. (2021) report  $T_p$  (peak) values between 60.29 and 63.80 °C and gelatinization enthalpy changes ( $\Delta H$ ) in the range between 7.95 and 8.88 J g<sup>-1</sup>, for starches of the genus *tuberosum*, as found in this study.

## Pasting Properties

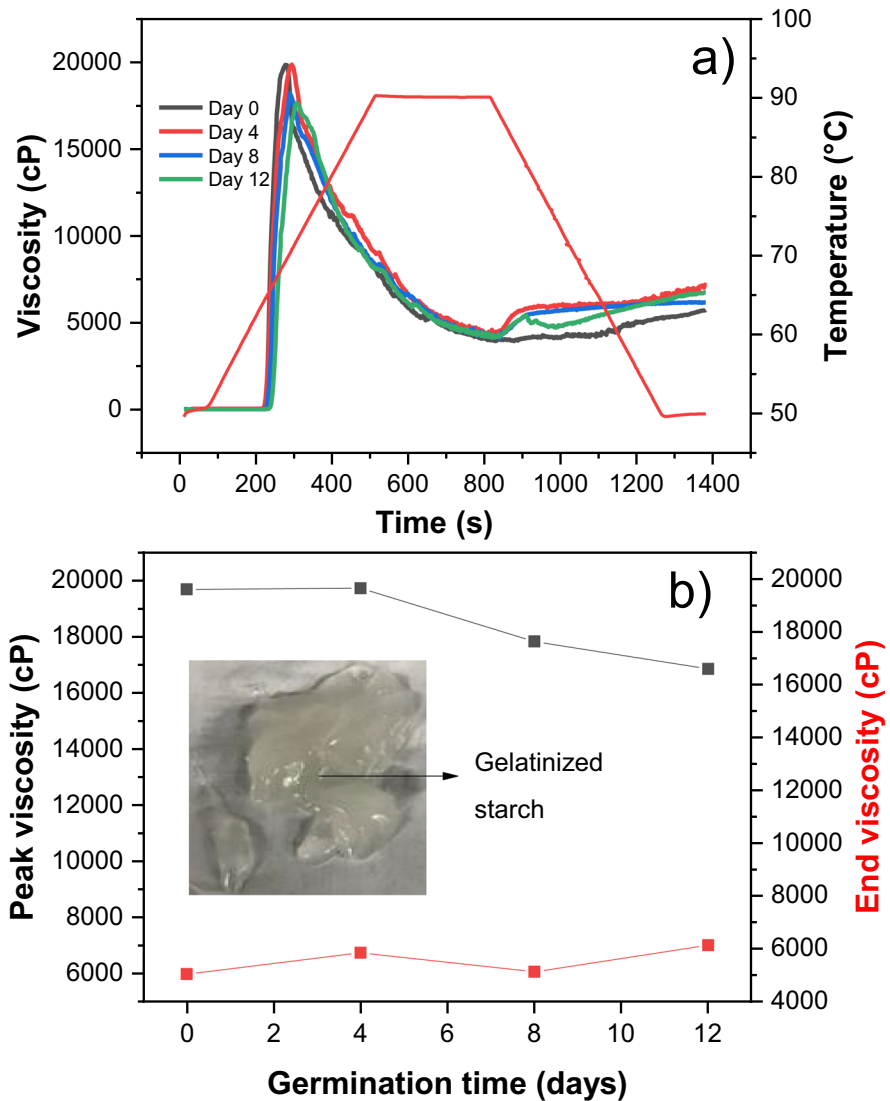
One of the main reasons for germination of seeds is to reduce the peak and end viscosity of the slurry to convert the original unmalted grain into a slurry with low end viscosity, which is formed by the hydroxylation of amylose and amylopectin, and to utilize the hexagonal nanocrystals in free D-glucose units that can ferment and produce alcohol. Grains such as corn, amaranth and sorghum have a high end viscosity, but the enzymatic process leads to the hydroxylation of amylose and amylopectin, decreasing the peak and end viscosity and making the slurry behave like a hydrogel (Pineda-Gómez et al. 2021).

Figure 6 shows the pasting profiles of starches, and it is important to recognize two points in these curves that serve to compare the differences between starches: (1) The peak viscosity, or the highest apparent viscosity reached, is the point at which the starch has lost its granular form and the leached amylose and amylopectin chains occupy more space and contribute to the increase in paste viscosity under heating conditions; (2) the final viscosity corresponds to the rearrangement of the chains during cooling and temperature reduction (Londoño-Restrepo et al. 2018).

Regarding the peak viscosity of the germinated starch of Creole potato, it is observed that it develops high viscosity peaks that decrease with increasing germination time, suggesting that the long amylose and amylopectin chains are fractionated, leading to an increase in reducing sugars and a decrease in apparent viscosity, although no enzymatic attack on the integrity of the starches is observed (Oseguera-Toledo et al. 2020).

Due to their viscosity profile, these potato varieties have great potential to be used as thickeners in various food formulations. The increase in viscosity upon cooling





**Fig. 6** Viscosity profiles of isolated Creole potato starch (a) and the changes in the peak and final viscosity at different times of germination (b)

indicates the ability of the starch to form gels by regrouping the leached granule chains. When the final viscosity is low, the starch–water dispersion behaves like a hydrogel, as in the case of starch from Creole potatoes (Fig. 6).

The SEM images show that the starch granules do not suffer any external damage as a result of the enzymatic process. However, the peak and final viscosity decreases and the slurry behaves like a hydrogel. The starch nanocrystals are normally dissolved by the heat and excess water in the slurry.

## Conclusions

The study of the short-term germination of this potato has shown that the starch grains do not show any surface or morphological changes associated with hydrolytic enzymes. This finding is confirmed by the fact that the functional properties of the isolated starch showed no significant changes. X-ray diffraction showed that the nanocrystals with hexagonal crystal structure do not undergo any changes during germination. This is an important indication, as these nanocrystals are the main source of energy storage. The gelatinization could be partly due to the solvation of the hexagonal crystals, but it is still an interesting phenomenon that requires further investigation.

**Acknowledgements** The authors would like to thank the University of Quindío, especially the Vice Rector for Research, for funding the project called “Evaluación de la potencialidad de leguminosas y tubérculos en la producción de bebidas alcohólicas fermentadas libres de gluten”.

**Funding** Open Access funding provided by Colombia Consortium. This work was financially supported by the Laboratorio Nacional de Caracterización de Materiales CFATA-UNAM, (Conhacyt-Mexico) at Campus Juriquilla.

## Declarations

**Ethics Approval** The authors have conducted themselves within the bounds of ethical behaviours. This is an original work. However, work and the words of other authors have been cited according to the references.

**Consent for Publication** All authors have read and approved the final version of the paper and consented to its publication.

**Conflict of Interest** The authors declare no competing interests.

**Open Access** This article is licensed under a Creative Commons Attribution 4.0 International License, which permits use, sharing, adaptation, distribution and reproduction in any medium or format, as long as you give appropriate credit to the original author(s) and the source, provide a link to the Creative Commons licence, and indicate if changes were made. The images or other third party material in this article are included in the article’s Creative Commons licence, unless indicated otherwise in a credit line to the material. If material is not included in the article’s Creative Commons licence and your intended use is not permitted by statutory regulation or exceeds the permitted use, you will need to obtain permission directly from the copyright holder. To view a copy of this licence, visit <http://creativecommons.org/licenses/by/4.0/>.


## References

- AOAC International (2006) Official methods of analysis of AOAC International, 20th edn. AOAC International, Rockville (USA)
- Agrimonti C, Visioli G, Bianchi R, Torelli A, Marmiroli N (2007) G1–1 and LeG1–1/LeG1–2 genes are involved in meristem activation during breakage of dormancy and early germination in potato tubers and tomato seeds. *Plant Sci* 173:533–541. <https://doi.org/10.1016/j.plantsci.2007.08.004>

- Cáceres M, Mestres C, Pons B, Gibert O, Amoros W, Salas E, Dufour D, Bonierbale M, Pallet D (2012) Physico-chemical characterization of starches extracted from potatoes of the group Phureja. *Starch/Stärke* 64:621–630. <https://doi.org/10.1002/star.201100166621>
- Choi I, Chun J, Choi HS, Park J, Kim NG, Lee SK, Park CH, Jeong KH, Nam JW, Cho J, Cho K (2020) Starch characteristics, sugars and thermal properties of processing potato (*Solanum tuberosum* L.) cultivars developed in Korea. *Am J Potato Res* 97:308–317. <https://doi.org/10.1007/s12230-020-09779-z>
- Contreras-Jiménez B, Del Real A, Millán-Malo BM, Gaytán-Martínez M, Morales-Sánchez E, Rodríguez-García ME (2019) Physicochemical changes in barley starch during malting. *J Inst Brew* 125:10–17. <https://doi.org/10.1002/jib.547>
- Daneri-Castro SN, Svensson B, Roberts TH (2016) Barley germination: Spatio-temporal consideration for designing and interpreting ‘omics’ experiments. *J Cereal Sci* 70:29–37. <https://doi.org/10.1016/j.jcs.2016.05.012>
- Delaplace P, Rojas-Beltran J, Frettinger P, du Jardin P, Fauconnier ML (2008) Oxylipin profile and antioxidant status of potato tubers during extended storage at room temperature. *Plant Physiol Biochem* 46:1077–1084. <https://doi.org/10.1016/j.plaphy.2008.09.001>
- Duarte-Delgado D, Narváez-Cuenca CE, Restrepo-Sánchez LP, Kushalappa A, Mosquera-Vásquez T (2021) Development and validation of a liquid chromatographic method to quantify sucrose, glucose, and fructose in tubers of *Solanum tuberosum* group Phureja. *J Chromatogr B* 975:18–23. <https://doi.org/10.1016/j.jchromb.2014.10.039>
- Dündar E, Yusuf T, Blaurock A (2009) Large scale structure of wheat, rice and potato starch revealed by ultra-small angle X-ray diffraction. *Int J Biol Macromol* 45(2):206–212. <https://doi.org/10.1016/j.ijbiomac.2009.05.002>
- Esquivel-Fajardo EA, Martínez-Ascencio EU, Oseguera-Toledo ME, Londoño-Restrepo SM, Rodríguez-García ME (2022) Influence of physicochemical changes of the avocado starch throughout its pasting profile: combined extraction. *Carbohydr Polym* 281:119048. <https://doi.org/10.1016/j.carbpol.2021.119048>
- Gasiński A, Kawa-Rygielska J (2022) Mashing quality and nutritional content of lentil and bean malts. *LWT - Food Sci Technol* 169:113927. <https://doi.org/10.1016/j.lwt.2022.113927>
- Gong B, Liu W, Tan H, Yu D, Song Z, Lucia LA (2016) Understanding shape and morphology of unusual tubular starch nanocrystals. *Carbohydr Polym* 151:666–675. <https://doi.org/10.1016/j.carbpol.2016.06.010>
- Grzesik M, Janas R, Stegłińska A, Kręgiel D, Gutarowska B (2022) Influence of microclimatic conditions during year-long storage of ‘Impresja’ potato tubers (*Solanum tuberosum* L.) on the emergence, growth, physiological activity and yield of plants. *J Stored Prod Res* 99:102033. <https://doi.org/10.1016/j.jspr.2022.102033>
- Gutiérrez-Cortez E, Hernández-Becerra E, Londoño-Restrepo SM, Rodríguez-García ME (2021) Physicochemical characterization of Amaranth starch insulated by mechanical separations. *Int J Biol Macromol* 177:430–436. <https://doi.org/10.1016/j.ijbiomac.2021.02.138>
- Juliano BO, Perez CM, Blakeney AB, Castillo T, Kongseree N, Laignelet B, Lapis ET, Murty VVS, Paule CM, Webb BD (1981) International cooperative testing on the amylose content of milled rice. *Starch-Stärke* 33:157–162. <https://doi.org/10.1002/star.19810330504>
- Lee JC, Tae-Wha M (2015) Structural characteristics of slowly digestible starch and resistant starch isolated from heat–moisture treated waxy potato starch. *Carbohydr Polym* 125:200–205. <https://doi.org/10.1016/j.carbpol.2015.02.035>
- Li C, Ohb SG, Lee DH, Baik HM, Chung HJ (2017) Effect of germination on the structures and physicochemical properties of starches from brown rice, oat, sorghum, and millet. *Int J Biol Macromol* 105:931–939. <https://doi.org/10.1016/j.ijbiomac.2017.07.123>
- Lucas-Aguirre JC, Giraldo-Giraldo GA, Cortés-Rodríguez M (2018) Effect of the spray drying process on the quality of coconut powder fortified with calcium and vitamins C D3 and E. *Adv J Food Sci Technol* 16:102–124. <https://doi.org/10.19026/ajfst.16.5943>
- Lucas-Aguirre JC, Giraldo-Giraldo GA, Cortés-Rodríguez M (2019) Stability during storage of coconut powder fortified with active components. *Biotecnol Sector Agropecuario Agroind* 17(2):66–76
- Lucas-Aguirre JC, Quintero-Castaño VD, Castañeda-Cano LF, Rodríguez-García ME (2023) Morphological, structural, chemical, vibrational, thermal, pasting, and functional changes in pea starch during germination process. *F1000Research* 12:940. <https://doi.org/10.12688/f1000research.136568.1>
- Lucas-Aguirre JC, Quintero-Castaño VD, Beltrán-Bueno M, Rodríguez-García ME (2024) Study of the changes on the physicochemical properties of isolated lentil starch during germination. *Int J Biol Macromol* 267:131468. <https://doi.org/10.1016/j.ijbiomac.2024.131468>

- Londoño-Restrepo SM, Rincón-Londoño N, Contreras-Padilla M, Millán-Malo BM, Rodríguez-García ME (2018) Morphological, structural, thermal, compositional, vibrational, and pasting characterization of white, yellow, and purple Arracacha Lego-like starches and flours (*Arracacia xanthorrhiza*). *Int J Biol Macromol* 113:1188–1197. <https://doi.org/10.1016/j.ijbiomac.2018.03.021>
- Mani F, Bettaieb T, Doudech N, Hannachi C (2014) Physiological mechanisms for potato dormancy release and sprouting: a review. *Afr Crop Sci J* 22(2):155–174
- Mueez-Ali S, Siddique Y, Mehnaz S, Bilal-Sadiq M (2023) Extraction and characterization of starch from low-grade potatoes and formulation of gluten-free cookies containing modified potato starch. *Heliyon* 9:e19581. <https://doi.org/10.1016/j.heliyon.2023.e19581>
- Neupane S, Sharma S, Sigdel S, Duwal R (2022) Effect of pre-sowing treatment of chemicals on sprouting of newly harvested potato at Kavre, Nepal. *Int J Agric Appl Sci* 3(2):108–113. <https://doi.org/10.52804/ijaas2022.3220>
- Oseguera-Toledo ME, Contreras-Jiménez B, Hernández-Becerra E, Rodríguez-García ME (2020) Physicochemical changes of starch during malting process of sorghum grain. *J Cereal Sci* 95:103069. <https://doi.org/10.1016/j.jcs.2020.103069>
- Pineda-Gomez PP, Mutis-González N, Contreras-Jimenez B, Rodríguez-García ME (2021) Physicochemical characterisation of starches from six potato cultivars native to the Colombian Andean region. *Potato Res* 64:21–39. <https://doi.org/10.1007/s11540-020-09462-0>
- Quintero-Castaño VD, Castellanos-Galeano FJ, Álvarez-Barreto CI, Lucas-Aguirre JC, Bello-Pérez LA, Rodríguez-García ME (2020) Starch from two unripe plantains and esterified with octenyl succinic anhydride (OSA): Partial characterization. *Food Chem* 315:126241. <https://doi.org/10.1016/j.foodchem.2020.126241>
- Rincón-Londoño N, Vega-Rojas LJ, Contreras-Padilla M, Acosta-Osorio AA, Rodríguez-García ME (2016) Analysis of the pasting profile in corn starch: structural, morphological, and thermal transformations, Part I. *Int J Biol Macromol* 91:106–114. <https://doi.org/10.1016/j.ijbiomac.2016.05.070>
- Rodríguez-García ME, Hernández-Landaverde MA, Delgado JM, Ramírez-Gutierrez CF, Ramírez-Cardona M, Millán-Malo BM, Londoño-Restrepo SM (2021) Crystalline structures of the main components of starch. *Curr Opin Food Sci* 37:107–111. <https://doi.org/10.1016/j.cofs.2020.10.002>
- Rojas-Molina I, Nieves-Hernandez MG, Gutierrez-Cortez E, Barrón-García OY, Gaytán-Martínez M, Rodríguez-García ME (2024) Physicochemical changes in starch during the conversion of corn to tortilla in the traditional nixtamalization process associated with RS2. *Food Chem* 439:138088. <https://doi.org/10.1016/j.foodchem.2023.138088>
- Thomas S, Vásquez-Benítez JD, Cúellar-Cepeda FA, Mosquera-Vásquez T, Narváez-Cuenca CE (2021) Vitamin C, protein, and dietary fiber contents as affected by genotype, agro-climatic conditions, and cooking method on tubers of *Solanum tuberosum* group Phureja. *Food Chem* 349:129207. <https://doi.org/10.1016/j.foodchem.2021.129207>
- Velásquez-Herrera JD, Lucas-Aguirre JC, Quintero-Castaño VD (2017) Physical-chemical characteristics determination of potato (*Solanum phureja* Juz. & Bukasov) starch. *Acta Agron* 66(3):323–330. <https://doi.org/10.15446/acag.v66n3.52419>
- Wu F, Chen H, Yang N, Wang J, Duan X, Jin Z, Xu X (2013) Effect of germination time on physicochemical properties of brown rice flour and starch from different rice cultivars. *J Cereal Sci* 58:263–271. <https://doi.org/10.1016/j.jcs.2013.06.008>
- Xing B, Teng C, Sun M, Zhang Q, Zhou B, Cui H (2021) Effect of germination treatment on the structural and physicochemical properties of quinoa starch. *Food Hydrocoll* 115:106604. <https://doi.org/10.1016/j.foodhyd.2021.106604>
- Xu M, Jin Z, Simsek S, Hall C, Rao J, Chen B (2019) Effect of germination on the chemical composition, thermal, pasting, and moisture sorption properties of flours from chickpea, lentil, and yellow pea. *Food Chem* 295:579–587. <https://doi.org/10.1016/j.foodchem.2019.05.167>
- Yang X, An J, Wang X, Wang L, Song P, Huang J (2023) Ar plasma jet treatment delay sprouting and maintains quality of potato tubers (*Solanum tuberosum* L.) by enhancing antioxidant capacity. *Food Biosci* 51:102145. <https://doi.org/10.1016/j.fbio.2022.102145>
- Zabrouskov V, Kumar G, Sychalla J, Knowles N (2002) Oxidative metabolism and the physiological age of seed potatoes are affected by increased  $\alpha$ -linolenate content. *Physiol Plant* 116:172–185. <https://doi.org/10.1034/j.1399-3054.2002.1160206.x>
- Zarate-Polanco L (2014) Extracción y caracterización de almidón nativo de clones promisorios de papa criolla (*Solanum tuberosum*, Grupo Phureja). *Rev Latinoam Papa* 18(1):1–24

## Authors and Affiliations

**Juan Carlos Lucas-Aguirre**<sup>1</sup>  · **Víctor Dumar Quintero-Castaño**<sup>1</sup> ·  
**Johan Sebastián Henao-Ossa**<sup>1</sup> · **Oscar Yael Barrón-García**<sup>2,3</sup> ·  
**Mario Enrique Rodríguez-García**<sup>2</sup>

✉ Juan Carlos Lucas-Aguirre  
jclucas@uniquindio.edu.co

✉ Mario Enrique Rodríguez-García  
marioga@fata.unam.mx

<sup>1</sup> Programa de Ingeniería de Alimentos, Facultad de Ciencias Agroindustriales, Universidad del Quindío, Quindío, Armenia, Colombia

<sup>2</sup> Departamento de Nanotecnología, Centro de Física Aplicada y Tecnología Avanzada, Universidad Nacional Autónoma de México, Campus Juriquilla, Querétaro, Qro., C.P 76230, México

<sup>3</sup> División Industrial, Universidad Tecnológica de Querétaro, Av. Pie de La Cuesta 2501, Nacional, 76148 Santiago de Querétaro, Qro, México